Parsons, S. M., & Raftery, M. A. (1969) *Biochemistry 8*, 4198–4205.
Phillips, D. C. (1967) *Proc. Natl. Acad. Sci. U.S.A. 57*, 484–495.
Rosenberg, S., & Kirsch, J. F. (1981) *Biochemistry 20*, 3196–3204.
Schachter, H. (1975) *Methods Enzymol. 41*, 3–10.
Sinnott, M. L., & Viratelle, O. M. (1973) *Biochem. J. 133*, 81–87.
Weber, J. P., & Fink, A. L. (1980) *J. Biol. Chem. 255*, 9030–9032.
Wohler, F., & Liebig, J. (1837) *Annu. Pharm. 22*, 1–24.

Energetics of Proline Racemase: Racemization of Unlabeled Proline in the Unsaturated, Saturated, and Oversaturated Regimes†

L. Mark Fisher,‡ W. John Albery,§ and Jeremy R. Knowles*
Department of Chemistry, Harvard University, Cambridge, Massachusetts 02138
Received September 20, 1984; Revised Manuscript Received December 19, 1985

ABSTRACT: The interconversion of L- and D-proline catalyzed by proline racemase has been studied. The entire time course of the approach to equilibrium has been followed. After a short time the product concentration is significant, and the reaction runs under reversible conditions. As the total substrate concentration is increased, the system moves from the unsaturated regime into the saturated regime. At very high substrate levels under the reversible conditions used, the rate constant for substrate racemization *falls*, as the system moves into the "oversaturated" regime. Here, the net rate of the enzyme-catalyzed reaction is limited by the rate of return of the free enzyme from the form that liberates product back to the form that binds substrate. The results are analyzed in terms of the simple mechanism

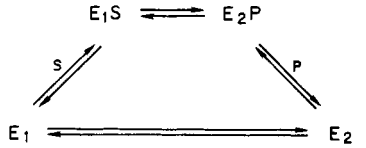

and illustrate the additional information that is available from reactions studied under reversible conditions. In the unsaturated region the value of the second-order rate constant k_U (equivalent to k_{cat}/K_m) is 9×10^5 M^{-1} s^{-1} in each direction. In the saturated region, $\vec{k}_{cat} = \overleftarrow{k}_{cat} = 2600$ s^{-1} and $K_m = 2.9$ mM. In the oversaturated region, the rate constant k_O is 81 M s^{-1}. The substrate concentration at which unsaturated and saturated terms contribute equally is 2.9 mM, and the substrate concentration at which saturated and oversaturated terms contribute equally is 125 mM.

This series of papers describes a number of experiments that have been designed to elucidate the mechanism and energetics of the reaction catalyzed by proline racemase. While amino acid racemases usually require the cofactor pyridoxal phosphate, which by aldimine formation with the α-amino group labilizes the proton at the chiral center, such a pathway is not followed for imino acids, and two elegant studies from Abeles' group (Cardinale & Abeles, 1968; Rudnick & Abeles, 1975) have illuminated the reaction pathway followed in the enzyme-catalyzed racemization of proline. Proline racemase is a dimeric enzyme of subunit M_r 38 000, and it contains one substrate binding site for every two subunits. It appears that one enzymic base abstracts the α-proton from the substrate's chiral center and the conjugate acid of another enzymic base protonates the substrate from the opposite side. The rate of enzyme-catalyzed tritium release from DL-[2-^{3}H]proline decreases with increasing proline concentration at high proline levels, which indicates that the substrate-derived proton is not released to the medium until after the release of the product

Scheme I: Reaction Scheme for an Isomerase (E) That Catalyzes the Interconversion of S and P

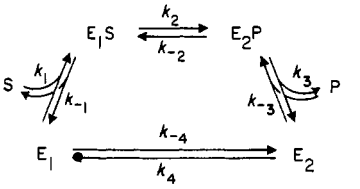

(Rudnick & Abeles, 1975). Since the rate of tritium release from L-[2-^{3}H]proline is not reduced by increasing L-proline concentration, the enzyme-bound proton derived from one enantiomer is only captured by the other enantiomer (Rudnick & Abeles, 1975). When the isomerization of unlabeled proline is studied in D_2O, the initial rate of deuterium incorporation into proline is the same as the rate of product formation in either direction (Cardinale & Abeles, 1968).

These experiments allowed Abeles and co-workers to conclude that there are two forms of the free enzyme, one that binds D-proline and one that binds L-proline. Release of product is faster than release of the substrate-derived proton, and release of this proton is at least as fast as the rate of interconversion of the two forms of the enzyme. At its simplest, therefore, proline racemase appears to fit Scheme I. The particular case of the racemase reaction has the further advantages of simplicity, of having overall symmetry, and of

† This work was supported by the National Science Foundation and Merck Sharp & Dohme.
‡ Present address: St. George's Hospital Medical School, University of London, London, England.
§ Present address: Department of Chemistry, Imperial College of Science and Technology, London SW7 2AY, England.

0006-2960/86/0425-2529$01.50/0

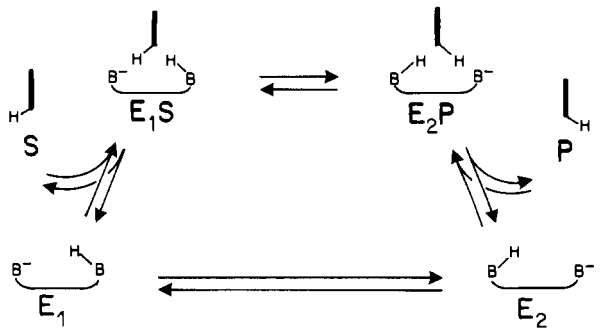

FIGURE 1: Proline racemase reaction. The two enzyme bases (B) catalyze the interconversion of the two enantiomers of proline (the proline ring is shown edge-on as a heavy bar).

being amenable to precise monitoring by the change in the optical rotation.

The work of Abeles allows us to elaborate the nature of E_1 and E_2 by consideration of the chemical changes effected by the enzyme. Abeles has proposed that there are two equivalent enzyme catalytic bases [which from chemical modification and protein chemical studies may be thiols (Rudnick & Abeles, 1975)] responsible for the catalyzed interconversion of the enzyme-bound enantiomers of proline (see Figure 1). On this basis, the two forms of the free enzyme must differ minimally by the state of protonation of the two catalytic bases (though there may, of course, be more substantial structural differences that result in L-proline only being accepted by E_1 and D-proline only being accepted by E_2). It will be clear that Figure 1 can accommodate the results from Abeles laboratory summarized above, provided that E_1 and E_2 do not interconvert by direct proton transfer between the two catalytic bases (this is a condition imposed by the fact that the release of a substrate-derived proton to the medium is at least as fast as the rate of interconversion of the two forms of the enzyme).

In this paper, we consider an enzyme-catalyzed reaction involving one substrate S, one product P, and two forms of the enzyme E_1 and E_2, as shown in Scheme I. In any reaction involving the enzyme-catalyzed conversion of S to P, it is unlikely that the enzyme will remain unchanged. Even though it is general practice to assume that the interconversion of E_1 and E_2 (Scheme I) is so rapid that the free enzyme can be treated as a single species, this assumption may be unjustified. Indeed, Cleland (1963) originally noted this possibility and pointed out that systems following such an "iso" mechanism would show noncompetitive inhibition by product.

An important feature of the experiments described is that the catalyzed reaction is not studied by removing the product in a coupled irreversible step: the system proceeds to equilibrium, and the sum of the concentrations of S and P remains constant. For this reason all the forward and backward reactions are included in Scheme I. We have previously distinguished between reversible and irreversible systems (Albery & Knowles, 1976). In a "reversible" system the enzyme converts S to P under conditions where the concentrations of S and P are close to their equilibrium values. In an "irreversible" system, the product P is rapidly removed by a coupled reaction; during the reaction the steady-state concentration of P is much smaller than its equilibrium value. Even though it is customary to study enzyme-catalyzed reactions in vitro under irreversible conditions, most such processes operate under reversible conditions in vivo. In the glycolytic pathway, for instance, only for three of the dozen or so enzymes are the substrate concentrations far displaced from their equilibrium values; the other nine enzymes operate near to reversible conditions even when the flux through the metabolic pathway is increased [e.g., 10^2-fold by the onset of flight, for insect flight muscle (Sacktor & Wormser-Shavit, 1966), or 10^3-fold by electrical tetanization of rat muscle (Hohorst et al., 1962)].

In the present paper we describe the kinetics of isomerization of L-proline and of D-proline catalyzed by proline racemase. The experiments are performed under reversible conditions where the approach to equilibrium is monitored continuously. Since after a short time the product is also present, it is the *net* flux that is measured when the reaction is followed under reversible conditions.

Experimental Procedures

Materials

D-Proline ($[\alpha]^{22}$ +85.7°) and L-proline ($[\alpha]^{22}$ −85.3°) were from Calbiochem and were recrystallized from absolute ethanol. Yeast extract and Bacto-Tryptone were from Difco Laboratories. DEAE-cellulose (DE-52) was from Reeve Angel, Sephadex G-150 was from Pharmacia, and cellulose (microcrystalline) was from Baker. Hydroxyapatite (calcium phosphate gel) was prepared by the method of Swingle and Tiselius (1951). All other chemicals were obtained from Fisher and were of the highest grade available. Buffer solutions were prepared with distilled–deionized–distilled water.

Proline racemase was isolated from *Clostridium sticklandii* (ATCC 12662). *Clostridium sticklandii* was stored at 37 °C in semisolid agar which was a modification of ATCC medium 43. The medium contained K_2HPO_4 (1.74 g), $CaCl_2$ (7 mg), $MgSO_4 \cdot 7H_2O$ (20 mg), $FeSO_4 \cdot 7H_2O$ (10 mg), L-arginine hydrochloride (2 g), L-lysine hydrochloride (2 g), yeast extract (4 g), sodium formate (2 g), ammonium chloride (2 g), agar (5 g), methylene blue (2 mg), and tap water to 1 L. This medium was autoclaved and then mixed with a sterile solution of $Na_2S \cdot 9H_2O$ (0.3 g in 10 mL of distilled H_2O), which was sufficient to generate the anaerobic conditions necessary for bacterial growth. Culture tubes were completely filled with this medium and capped tightly to exclude atmospheric oxygen. Bacteria were stored as stabs 37 °C. The oxidation state of the stabs was indicated by the color of the medium: brown indicating reducing conditions and green indicating oxidizing conditions. The growth medium contained K_2HPO_4 (1.74 g), tryptone (22.2 g), yeast extract (5 g), sodium formate (1.5 g), and tap water to 1 L. The medium was autoclaved, and then a sterile solution of $Na_2S \cdot 9H_2O$ (0.6 g in 20 mL of distilled water) was added. For large-scale growth, bacteria were transferred from semisolid agar to growth medium (30 mL) contained in two 20-mL tubes. The tubes were incubated at 37 °C for 48 h, and the cell cultures (30 mL) were then added to 2 L of growth medium. The culture was left at 37 °C for 24 h and then used to inoculate 20 L of growth medium. After being incubated at 37 °C for 24 h, the bacterial culture was transferred to a fermenter containing 170 L of growth medium. After stirring at 37 °C for 18 h, the bacteria were harvested. The packed cells (415 g) were stored frozen at −20 °C.

The enzyme was purified by a modification of the method of Cardinale and Abeles (1968).

(*a*) *Sonic Extract.* Cells of *Clostridium sticklandii* (215 g) were thawed and suspended in 0.01 M tris(hydroxymethyl)aminomethane hydrochloride (Tris-HCl)[1] buffer, pH 8.7 (400 mL) at 4 °C. The suspension was sonicated (using a Branson Model W350 sonifier) for 15 min, keeping the temperature of the sonicate at <10 °C. The black sonicate was centrifuged at 16300*g* for 1 h. The pellet was washed with

[1] Abbreviations: Tris-HCl, tris(hydroxymethyl)aminomethane hydrochloride; EDTA, (ethylenedinitrilo)tetraacetic acid.

Table I: Purification of Proline Racemase from *Clostridium sticklandii*[a]

procedure	volume (mL)	total units	units/mg of protein[b]	yield (%)	purification
extract	2731	35 250	0.85	100	1
protamine sulfate	2780	22 000	0.59		
ammonium sulfate	204	17 100	1.1	48	1.25
70 °C heating	493	13 300	1.4	37	1.66
DEAE column	500	12 700	88	36	103
hydroxylapatite column	11.5	2 900	330	8.3	386
second G-150[c] column	0.8	1 100	742	3	869

[a] On the basis of 415 g of cells. [b] Protein concentrations were determined by $A_{280\,nm}$, on the basis that $1.65A_{280nm}^{10mm} \equiv 1$ mg/mL. [c] Pooled fractions stored at 4 °C in Tris-HCl buffer.

0.01 M Tris-HCl buffer, pH 8.7 (400 mL), and spun at 16300*g* for 1 h. The combined supernatants had an OD_{280}/OD_{260} of 0.6.

(*b*) *Protamine Sulfate.* The sonic extract (960 mL) was stirred with 2% protamine sulfate (200 mL) for 10 min at 4 °C, and the solution was then centrifuged at 12000*g* for 1 h. The pellet was discarded.

(*c*) *Ammonium Sulfate Precipitation.* To the supernatant (960 mL) was added ammonium sulfate (470 g) (low in heavy metals), and the mixture was stirred at 4 °C for 1 h before centrifuging at 12000*g* for 30 min. The pellet was resuspended in 0.01 M Tris-HCl buffer, pH 8.7 (400 mL), containing ammonium sulfate (140 g). The suspension was stirred at 4 °C for 17 h and centrifuged at 12000*g* for 30 min. The crude enzyme was precipitated from the supernatant with ammonium sulfate (264 g L^{-1}). The precipitate was dissolved in 0.05 M Tris-HCl, pH 8.7 (70 mL).

Steps a–c were repeated with a second batch of cells (200 g), and the two ammonium sulfate fractions were combined.

(*d*) *Heat Step.* The pH of the ammonium sulfate fraction was adjusted to 9 with 1 M Tris (~300 mL), and the solution was heated to 70 °C for 17 min. Denatured protein was removed by centrifugation, and the supernatant (493 mL) was dialyzed for 48 h against 0.1 M Tris-HCl, pH 7.5.

(*e*) *DEAE-cellulose Chromatography.* The dialyzed protein solution was applied to a column (4.5 cm × 4 cm) of DEAE-cellulose (DE-52) that had been preequilibrated with 0.1 M Tris-HCl, pH 7.5. The column was washed with starting buffer (250 mL) and eluted with a linear gradient (1 L plus 1 L) of Tris-HCl, pH 7.5 (0.1–0.3 M). Fractions (20 mL) were collected, and those containing proline racemase activity were pooled. The solution (500 mL) was brought to 90% saturation with ammonium sulfate. The precipitate was spun down and resuspended in 0.01 M potassium phosphate buffer, pH 6.8 (5 mL). This solution was dialyzed against 0.01 M potassium phosphate buffer, pH 6.8.

(*f*) *Hydroxylapatite Chromatography.* A calcium phosphate column (4.5 cm × 4 cm) was prepared from a mixture of freshly made calcium phosphate suspension (40 mL, defined) and cellulose (microcrystalline, 15 g). The column was washed overnight with 0.01 M potassium phosphate buffer, pH 6.8 (250 mL), and the dialyzed enzyme sample was applied. The column was then washed with 0.01 M potassium phosphate buffer, pH 6.8 (250 mL), followed by a linear gradient (300 mL plus 300 mL) of potassium phosphate, pH 6.8 (0.01–0.06 M). Fractions of 6 mL were collected, and those containing proline racemase activity were pooled and concentrated on a column (2 cm × 2 cm) of DE-52 equilibrated with 0.1 M Tris-HCl, pH 7.5. The enzyme was eluted with 0.4 M Tris-HCl, pH 7.5, and further concentrated by vacuum dialysis.

(*g*) *Sephadex G-150 Chromatography.* Proline racemase in 250 mM Tris-HCl buffer, pH 8.5 (400 μL), was applied to a column (27 cm × 1.5 cm) of Sephadex G-150 equilibrated with 250 mM Tris-HCl buffer, pH 8.5. The column was eluted with the same buffer, and fractions of 0.5 mL were collected. Fractions containing proline racemase with a specific activity of ≥800 units/mg were pooled and concentrated (to 0.3 mL) in a collodion membrane. The enzyme was then chromatographed on a second column (27 cm × 1.5 cm) of Sephadex G-150. Fractions from the column were examined by polyacrylamide gel electrophoresis, and those containing proline racemase ≥90% pure (based on densitometer scans) were pooled. The results of the purification procedure are shown in Table I.

Methods

Optical rotation measurements were made on a Perkin-Elmer 141 polarimeter. pH measurements were made on a Radiometer PHM64 research pH meter. Conductivity measurements were made on a Radiometer CDM3 conductivity meter.

Concentrations of D-proline and of L-proline in kinetic experiments were determined from the optical rotation of the solution at 365 nm in a cell of 10-cm path length, thermostated at 37 °C. An optical rotation of 1° is equivalent to a proline concentration of 33.26 mM.

Enzyme activity was assayed either by observing the optical rotation of a solution of L-proline after incubation at 37 °C with the racemase at pH 8.0, followed by quenching with trichloroacetic acid (Cardinale & Abeles, 1968), or by incubating L-proline (80 mM) in 200 mM Tris-HCl, pH 8.0 (1 mL) containing 2-mercaptoethanol (20 mM) and EDTA (8 mM) at 37 °C. Proline racemase (200 μL, 0.1–0.2 unit in Tris-HCl buffer) was added and the solution transferred to an optical rotation cell of 10-cm path length, jacketed at 37 °C. The optical rotation of the solution at 365 nm was followed with time. One unit of proline racemase is defined as the amount of enzyme required to convert 1 μmol of L-proline to D-proline per minute at 37 °C under these conditions.

In all the kinetic studies, the racemization of L-proline and of D-proline catalyzed by proline racemase was studied at 37 °C in 200 mM Tris-HCl buffer, pH 8.0, containing 2-mercaptoethanol (20 mM) and EDTA (8 mM), by monitoring the optical rotation at 365 nm. Owing to the relative insensitivity of the optical rotation method, measurements were restricted to proline concentrations greater than or equal to 1.5 mM.

The kinetic experiments were run under essentially the same conditions as used by Abeles and his group (Cardinale & Abeles, 1968; Rudnick & Abeles, 1975), thus allowing direct comparison of the kinetic results with their experiments.

Theory

We derive here the kinetic equations for Scheme I, following the methodology and notation used for the general treatment (Albery & Knowles, 1986). To simplify the algebra, we use

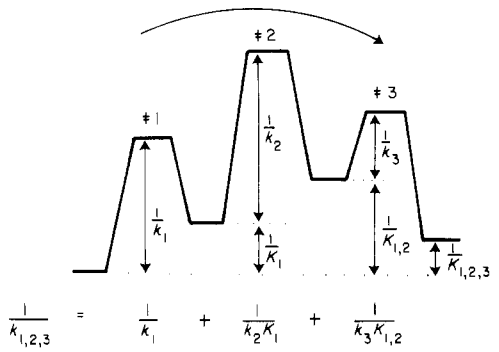

FIGURE 2: Free energy diagram of a three-step process. Each term in the reciprocal form of the expression for a composite rate constant $k_{1,2,3}$ is associated with one of the three transition states (see eq 1).

"composite" rate constants and apply uniform flux theory in the derivation. First, a composite rate constant describes the rate of reaction over a sequence of transition states, and if written as the sum of reciprocal rate and equilibrium constants, each term describes the free energy difference between the *n*th transition state and the original reactant. This is illustrated for a three-step sequence in Figure 2. In the forward direction, we have

$$\frac{1}{k_{1,2,3}} = \frac{1}{k_1} + \frac{1}{k_2K_1} + \frac{1}{k_3K_{1,2}} \tag{1}$$

and for the reverse reaction

$$\frac{1}{k_{-3,2,1}} = \frac{1}{k_{-3}} + \frac{K_3}{k_{-2}} + \frac{K_{2,3}}{k_{-1}}$$

Analogously, we may write, for the overall equilibrium constant $K_{S,P}$ for the interconversion of S and P in Scheme I (which for a racemase is unity):

$$K_{S,P} = K_{1,2,3}K_4 = 1.0$$

Second, we use the uniform flux approach, which assumes that the net fluxes of material through each transition state of an unbranched reaction sequence are equal. This is equivalent to the more common steady-state approximation and similarly requires that the enzyme concentration is much smaller than the substrate concentration. As is clear from what follows, this approach reduces the complexity of the kinetic expressions.

We now write the equations for the net fluxes f round the cycle shown in Scheme I:

$$f = k_1e_1 \cdot s - k_{-1}e_1s \tag{2}$$

$$f = k_2e_1s - k_{-2}e_2p \tag{3}$$

$$f = k_3e_2p - k_{-3}e_2 \cdot p \tag{4}$$

$$f = k_4e_2 - k_{-4}e_1 \tag{5}$$

where the lower case letters e, s, and p are used to denote the concentrations of enzyme, substrate, and product species, respectively. The sum of the concentrations of the different forms of the enzyme must always equal the total enzyme concentration, e_Σ:

$$e_\Sigma = e_1 + e_1s + e_2p + e_2 \tag{6}$$

Now, from eq 2–6, we eliminate the four unknown enzyme concentrations to obtain

$$\frac{e_\Sigma(s-p)}{f} = \underbrace{\frac{1+K_4^{-1}}{k_{1,2,3}}}_{\text{unsaturated term}} + \underbrace{\frac{s}{k_{cat^+}} + \frac{p}{k_{cat^-}}}_{\text{saturated terms}} + \underbrace{\frac{sp(K_{2,3}^{-1} + K_3^{-1})}{k_4}}_{\text{oversaturated term}} \tag{7}$$

where

$$\frac{1}{k_{cat^+}} = \frac{1}{k_{2,3}} + \frac{1}{k_3} + \frac{1}{k_4} \tag{8}$$

and

$$\frac{1}{k_{cat^-}} = \frac{1}{k_{-1}} + \frac{1}{k_{-2,1}} + \frac{1}{k_{-4}} \tag{9}$$

For a reaction under *irreversible* conditions where P is removed by a coupling reaction so that $p = 0$, eq 7 reduces to

$$\frac{e_\Sigma s}{f} = \underbrace{\frac{1+K_4^{-1}}{k_{1,2,3}}}_{\text{unsaturated term}} + \underbrace{\frac{s}{k_{cat^+}}}_{\text{saturated term}} \tag{10}$$

which is analogous to a reciprocal form of the classical Michaelis–Menten equation. In eq 10, the unsaturated term describes the situation at low substrate concentration where the flux is determined by reaction from the most stable form of the enzyme E_1 or E_2 (described by $1 + K_4^{-1}$) over the highest barrier in the sequence of transition states 1–3 (described by $k_{1,2,3}$: see Figure 2). This term is equivalent to K_m/k_{cat}. The rate-limiting free energy difference is that between the lowest *free* form of the enzyme and the highest *bound* transition state. The saturated term in eq 10 is determined by k_{cat^+}, which is defined in eq 8. Here the terms $k_{2,3}^{-1}$ and k_3^{-1} relate to free energy differences between *bound* forms of the enzyme (E_1S and E_2P) and *bound* transition states (2 and 3). The third term in eq 8, k_4^{-1}, introduces the possibility that the interconversion of the two forms of the free enzyme may limit the turnover of the enzyme round the cycle shown in Scheme I.

If the reaction is under *reversible* conditions, eq 7 applies, and it is clear that, in addition to the unsaturated term and the two saturated terms, there is a final term in sp. It is possible that the reaction rate may be limited by the interconversion of the two enzyme forms, and if both S and P are present (i.e., under reversible conditions) and high, this last term in eq 7 may dominate the rate expression. The flux is then governed by the conversion of the lowest *bound* enzyme form (E_1S or E_2P) over the highest *free* enzyme transition state (4). This kinetic region we call *oversaturation*.

In summary, there are three kinetic regimes for a system that follows the simple Scheme I, which differ in the nature of the most stable species and of the highest transition state. In the unsaturated regime we go from a *free* enzyme form over a *bound* transition state. In the saturated regime we go either from a *bound* intermediate over a *bound* transition state or from a *free* enzyme form over a *free* transition state. In the oversaturated region we go from a *bound* intermediate over a *free* transition state. These relationships are illustrated in Figure 3. It is important to recognize that saturated behavior can arise not only from the classical interconversion of bound enzyme species (bound state saturated) but also from the rate-limiting interconversion of forms of the free enzyme (free state saturated). A fuller discussion can be found in Albery and Knowles (1986).

We may now use eq 7 to obtain an expression that describes the time course of the racemization of substrate S. Using

$$f = -\frac{ds}{dt} = \frac{dp}{dt}$$

and

$$s + p = c$$

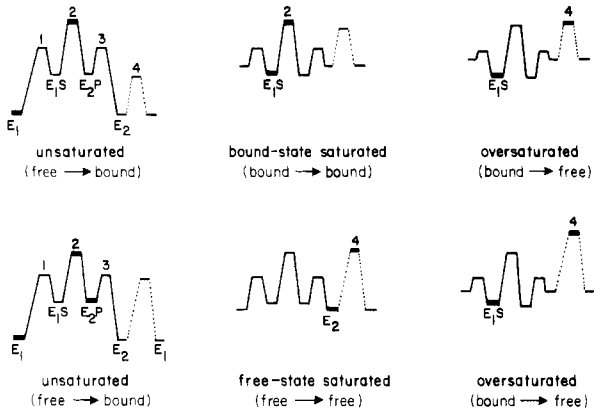

FIGURE 3: Free energy profiles illustrating the kinetic regimes for an enzyme reaction following Scheme I. The free energy changes for the interconversion of substrate S and product P are shown as a solid line; the changes for the interconversion of the free enzyme forms E_1 and E_2 are shown by the dashed line. The states that determine the rate of reaction in the different regimes are shown by heavy bars. Upper row, a system that is bound state saturated; lower row, a system that is free state saturated.

we may integrate with the boundary condition that $s = c$ at $t = 0$ to give

$$\frac{e_\Sigma t}{c} = -k_I^{-1} \ln [2s/c - 1] + \frac{(1 - s/c)}{2}\left(\frac{1}{k_{cat^+}} - \frac{1}{k_{cat^-}}\right) - \frac{s(1 - s/c)}{4k_O} \quad (11)$$

where

$$k_I^{-1} = \frac{1}{4}\left(\frac{2}{k_U c} + \frac{1}{k_{cat^+}} + \frac{1}{k_{cat^-}} + \frac{c}{2k_O}\right) \quad (12)$$

$$k_U = k_{1,2,3}/(1 + K_4^{-1}) \quad (13)$$

$$k_O = k_4/(K_3^{-1} + K_{2,3}^{-1}) \quad (14)$$

Inspection of eq 11 shows that toward the end of the racemase reaction when s is approaching $c/2$, the dominant term on the right-hand side is the logarithmic term. Under these conditions the system is close to equilibrium, the reaction is first order, and the observed rate constant k_F will be

$$k_F = k_I e_\Sigma / c \quad (15)$$

from which we derive the first-order rate constant k_I, which is independent of the enzyme concentration.

How does k_I depend upon the substrate concentration? At low substrate levels, it is clear from eq 12 that k_I is dominated by the *unsaturated* second-order rate constant, k_U, defined in eq 13, which is equivalent to the familiar parameter k_{cat}/K_m. As the concentration of substrate rises, k_I becomes dominated by the *saturated* first-order terms in k_{cat^+} and k_{cat^-} in eq 12, and finally, at very high substrate levels, k_I becomes dominated by the *oversaturated* zero-order rate constant, k_O, defined in eq 14. In the general case, the ratio of k_{U^+} for the reaction of S to P and k_{U^-} for the reaction of P to S will obey the Haldane relation, $k_{U^+}/k_{U^-} = K_{S,P}$, and we have shown (Albery & Knowles, 1986) that the ratio of the oversaturated rate constants also obeys this relation. But since for a racemase $K_{S,P} = 1.0$, k_U is the same whether S is reacting to P or P is reacting to S. Analogously, there is only one value of k_O for a racemase.

Finally, returning to eq 11, we can see that the two non-logarithmic terms on the right-hand side of this equation describe the departure from first-order kinetics that may be observed at the start of the reaction. The k_{cat} term and the k_O term may be significant in the saturated and oversaturated regions, respectively.

Table II: Kinetic Parameters for the Interconversion of L- and D-Proline Catalyzed by Proline Racemase

parameter	source	value
k_U (M^{-1} s^{-1})	gradient of Figure 7	9.7 (±1.1) × 10^5
$k_{cat^+}^{-1} + k_{cat^-}^{-1}$ (s)	intercept of Figure 7	8.2 (±1.0) × 10^{-4} [a]
$k_{cat^+}^{-1} + k_{cat^-}^{-1}$ (s)	intercept of Figure 9	8.6 (±0.4) × 10^{-4} [b]
k_O (M s^{-1})	gradient of Figure 9	84 ± 6
k_O (M s^{-1})	gradient of Figure 10	75 ± 4
k_{cat^+} (L) (s^{-1})	Lineweaver–Burk plot[c]	2000
k_{cat^-} (D) (s^{-1})	Lineweaver–Burk plot[c]	2000
K_m (L) (mM)	Lineweaver–Burk plot[c]	2.9
K_m (D) (mM)	Lineweaver–Burk plot[c]	2.5

[a] If $k_{cat^+} = k_{cat^-}$, this gives a value for k_{cat} of 2400 s^{-1}. [b] If $k_{cat^+} = k_{cat^-}$, this gives a value for k_{cat} of 2300 s^{-1}. [c] Lineweaver–Burk plot of the initial velocities.

Results and Discussion

We start by comparing experiments carried out at different substrate concentrations, and in order to present the results from different experiments together on the same graph, it is convenient to define a normalized time scale t_n, where

$$t_n = te_\Sigma/c \quad (16)$$

The interconversion of S and P is followed by measuring the optical rotation, and we define the dimensionless parameter λ as

$$\lambda = (s - p)/c \quad (17)$$

which is related to the optical rotation measured experimentally by

$$\lambda = |\alpha_t|/(|[\alpha]|c)$$

where α_t is the measured rotation at time t and $[\alpha]$ is the specific rotation for the L- or D-proline under the same conditions. Substitution of eq 16 and 17 into eq 11 gives

$$t_n = -\frac{\ln \lambda}{k_I} \pm \frac{1}{4}\left(\frac{1}{k_{cat^+}} - \frac{1}{k_{cat^-}}\right)(1 - \lambda) - \frac{c}{16k_O}(1 - \lambda^2) \quad (18)$$

where the plus sign relates to reactions from S to P and the minus sign relates to reactions from P to S.

We may now plot the experimental results for the variation of optical rotation (scaled, as λ) with time (scaled, as t_n) for the whole range of substrate concentrations, as shown for L-proline in Figure 4. A set of similar curves is obtained for the racemization of D-proline. Figure 4A shows the results for substrate concentrations (c) of 15.6 mM and below. Because, in obtaining λ and t_n, we divided *both* the optical rotation and the time by c (the total concentration of substrates), the initial gradients of the plots in Figure 4A correspond to the initial velocities of the reactions. As the substrate concentration increases from 1.6 to 15.6 mM, the *initial* velocity increases. The data for higher substrate concentrations (above 15.6 mM) are plotted in Figure 4B. At these higher concentrations the initial velocity becomes independent of substrate concentration, as expected for saturation of the enzyme. Since at very short times the reaction is essentially irreversible, these initial velocities can be treated classically and k_{cat} and K_m values obtained from a double-reciprocal plot. The Lineweaver–Burk plots for reactions starting with D-proline and with L-proline are almost identical, and the values of k_{cat} and K_m derived from these plots are listed in Table II. These

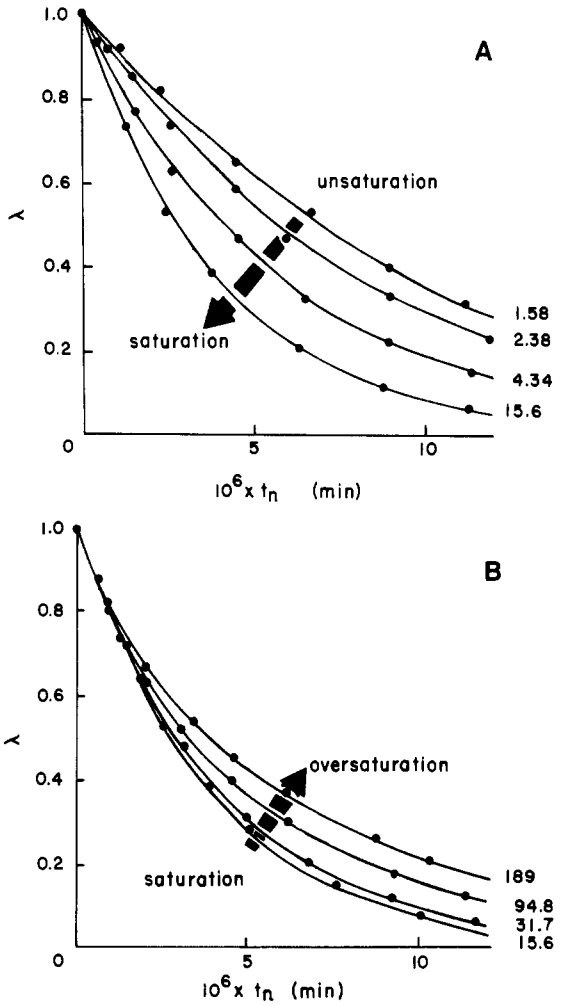

FIGURE 4: Kinetics of the racemization of L-proline catalyzed by proline racemase at low (A) and high (B) substrate concentrations. Initial substrate concentrations (c) (in mM) are shown by each curve. λ = (optical rotation at time t)/(initial optical rotation), and $t_n = te_\Sigma/c$. The enzyme concentrations (e_Σ) were 19.4 and 1.77 nM for initial proline concentrations of $\geq$15.6 and $\leq$4.34 mM, respectively. All reactions were run in 200 mM Tris-HCl buffer, pH 8.0, 37 °C.

values, where only the initial part of the reaction was used, are, however, less precise than the parameters that derive from analysis of the whole reaction time course described below.

Inspection of Figure 4B reveals, however, a new phenomenon. After the first phase of the reactions (all of which proceed at the same initial rate), the rate of proline equilibration *decreases* as the substrate concentration increases (see the arrow in Figure 4B). A number of trivial explanations for the slowing down of the racemization rate at high proline concentrations may be quickly eliminated. First, the phenomenon is not due to an ionic strength effect caused by increasing the concentration of proline, since the rates of racemization of proline (15 mM) in the presence and absence of sodium chloride (175 mM) are essentially identical. Second, the effect is not due to inhibition by excess substrate, since, under initial velocity conditions (i.e., before significant amounts of product have accumulated), the rates of racemization follow Michaelis–Menten kinetics and give linear Lineweaver–Burk plots in both the forward and reverse directions. The absence of substrate inhibition is also evident from the results of Rudnick and Abeles (1975) on the rates of ^3H release from L-[2-^{3}H]proline catalyzed by the racemase. The initial rates of tritium release exhibit saturation kinetics at high concentrations of L-[2-^{3}H]proline, which is consistent with the absence

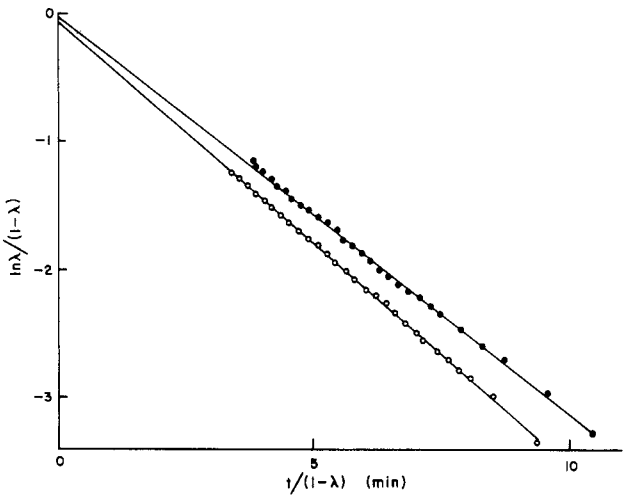

FIGURE 5: Plot of $\ln(\lambda)/(1-\lambda)$ vs. $t/(1-\lambda)$ for the racemization of 15.6 mM L-proline (●) and of 15.7 mM D-proline (○) catalyzed by proline racemase. Readings of the optical rotation were taken for approximately 10 min, starting 1 min after the addition of enzyme.

of inhibition by excess substrate.

A classical explanation for the curvature in the plots in Figure 4B is product inhibition: the rate decreases because of the competitive binding of the accumulated product at the active site. Inspection of eq 12 shows that, in the saturated region, k_I depends on k_{cat^+} and k_{cat^-} unmodified by any substrate concentration term. So although product inhibition could explain the curvature of the plots in Figure 4B, it cannot explain why successively higher concentrations of substrate lead to slower and slower reaction at long times. Classical competitive product inhibition would require the normalized data in Figure 4B to lie on a single curve, whereas noncompetitive product inhibition will produce the observed behavior. How can noncompetitive product inhibition arise for an enzyme such as a racemase, which has only one product? The phenomenon can be explained if there are two forms of the free enzyme, as follows. When the racemase reaction is followed under reversible conditions, the *net* conversion of substrate to product is measured, and this net flux depends upon the rate at which the "product" form of the enzyme (E_2, Scheme I) can convert to the "substrate" form of the enzyme (E_1, Scheme I). *Only* a conversion of E_2 to E_1 completes an enzyme turnover and produces a net flux of substrate from S to P. At very high concentrations of S and P, the concentrations of free E_2 (and free E_1) are very small, and most of the enzyme spends its time shuttling to and fro over the upper pathway of Scheme I. At these high substrate levels, therefore, the enzyme has less and less chance to complete a turnover, and the net conversion of S to P falls. This is oversaturation. In terms of eq 12, as c rises, the k_O term becomes increasingly important, and the rate of substrate equilibration, k_I, falls.

The whole time course of the reactions shown in Figure 4 can be analyzed by using eq 18. We first explore the second term of eq 18. This term dominates in the saturated region, which (from Figures 4A,B) is seen at a substrate concentration of about 16 mM. At this concentration we may neglect the oversaturated term in eq 18, and rearrangement then gives

$$\frac{\ln \lambda}{1-\lambda} = -k_I\left(\frac{e_\Sigma}{c}\right)\left(\frac{t}{1-\lambda}\right) \pm \frac{k_I}{4}\left(\frac{1}{k_{cat^+}} - \frac{1}{k_{cat^-}}\right) \quad (19)$$

Figure 5 shows the data at a substrate concentration of 16 mM plotted according to this equation for the reaction in each direction. The vertical intercepts of these linear plots are close to the origin, showing that k_{cat^+} is nearly equal to k_{cat^-}. From

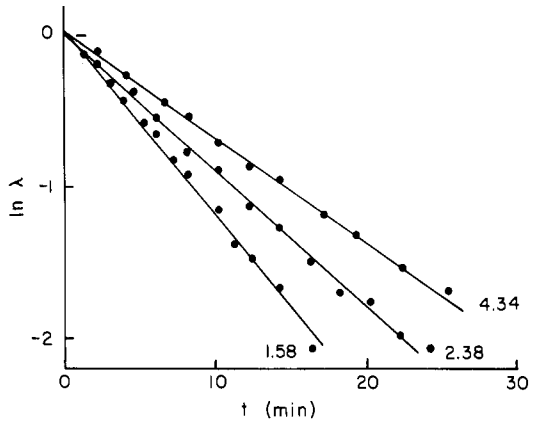

FIGURE 6: Plot of ln λ vs. t for the racemization of low concentrations of L-proline. Only a few representative data points are plotted. Initial substrate concentrations (in mM) are shown by each line.

the values of these intercepts and the values of k_I obtained from the gradients, we find that

$$\frac{1/k_{cat^+} - 1/k_{cat^-}}{1/k_{cat^+} + 1/k_{cat^-}} = 0.01 \pm 0.02 \qquad (20)$$

It is clear that within experimental error, $k_{cat^+} = k_{cat^-}$. This conclusion is supported by the almost identical Lineweaver–Burk plots obtained from the initial velocities from Figure 4 and the corresponding data for D-proline. Such symmetry in the energetics of the catalyzed reaction is perhaps not surprising for a racemase that catalyzes the interconversion of two enantiomers. If the system is bound state saturated, then the identity of k_{cat} values implies a symmetry in the catalytic steps; E_1S and E_2P have the same free energy and $K_2 = 1$. On the other hand, if the system is free state saturated, then the identity of the k_{cat} values implies that $k_4 = k_{-4}$ and that E_1 and E_2 have the same free energy.

Returning to eq 18, we now consider the results at low substrate concentrations (see Figure 4A) and can now neglect both the second (saturated) and the third (oversaturated) terms, to write

$$\ln \lambda = -k_1(e_\Sigma/c)t \qquad (21)$$

Figure 6 shows plots of the data at low substrate concentrations according to this equation. Reasonable straight lines are obtained, and the values of k_I are found from the gradients.

Taking the values of k_I from Figures 5 and 6, we may plot k_I^{-1} vs. c^{-1} in accord with eq 12 (neglecting the oversaturated term in k_O since these experiments only relate to the unsaturated and saturated regions). This plot is shown in Figure 7, from which we obtain values of k_U and of $(1/k_{cat^+} + 1/k_{cat^-})$ from the gradient and intercept, respectively. These data are collected in Table II.

Finally, we examine the results shown in Figure 4B that relate to the highest substrate concentrations. Since we know that $k_{cat^+} = k_{cat^-}$, eq 18 reduces to

$$\frac{\ln \lambda}{1 - \lambda^2} = -k_1\left(\frac{e_\Sigma}{c}\right)\left(\frac{t}{1 - \lambda^2}\right) - \frac{k_I c}{16k_O} \qquad (22)$$

In Figure 8 are plotted the results for reactions at high substrate concentrations, according to eq 22. Good straight lines are again obtained, from the gradients of which we obtain values of k_I. A plot of k_I^{-1} vs. c for these high substrate concentrations can now be made (Figure 9) in accord with eq 12 (the unsaturated term in k_U being insignificant at these high substrate levels). Values of k_O and of $(1/k_{cat^+} + 1/k_{cat^-})$ are obtained from the gradient and intercept of this plot and are listed in Table II. The intercepts of Figure 8 yield values of

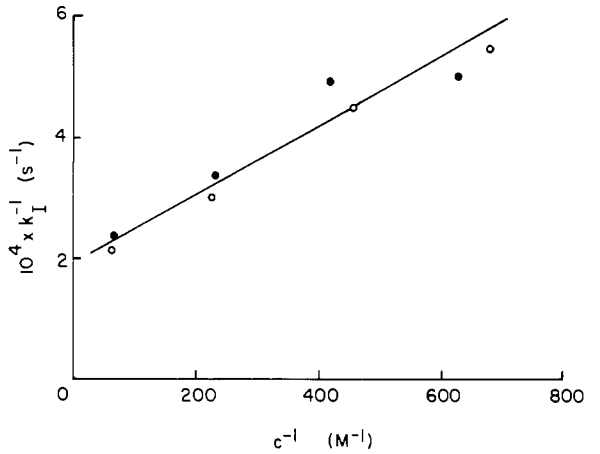

FIGURE 7: Plots of k_I^{-1} vs. c^{-1} for the racemization of L-proline (●) and of D-proline (○). The values of k_I^{-1} derive from the data of Figure 6. Only reactions where c is ≤15.6 mM are plotted.

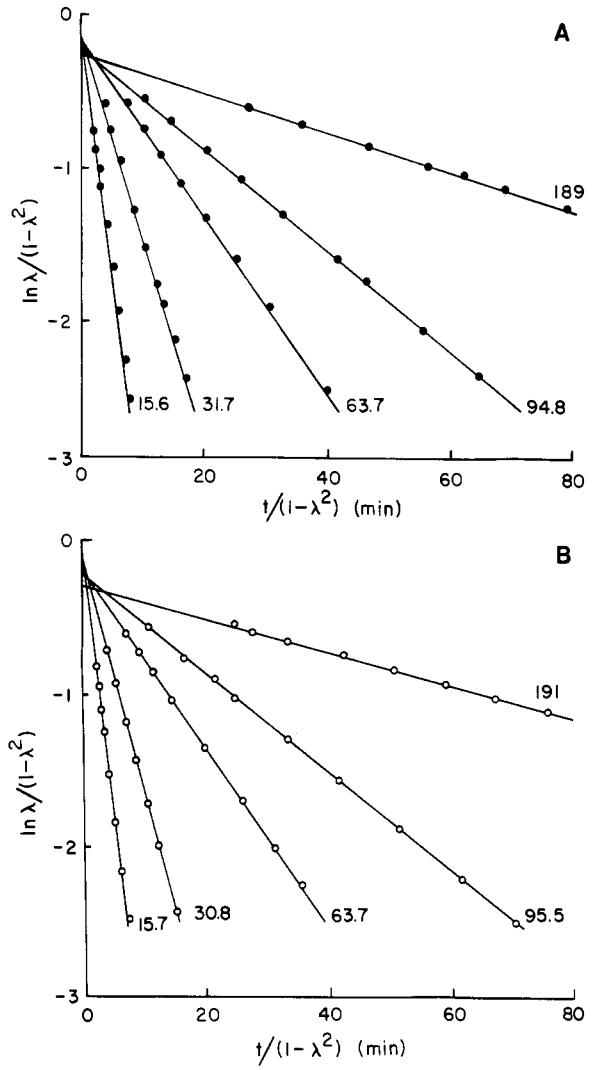

FIGURE 8: Plots of $\ln(\lambda)/(1 - \lambda^2)$ vs. $t/(1 - \lambda^2)$ for the racemization of L-proline (A) and of D-proline (B). The substrate concentrations (in mM) are shown. λ and t are as defined in the legend to Figure 4. Only reactions where c is ≥15.6 mM are plotted. The enzyme concentration was in all cases 19.4 nM.

$k_I c/16k_O$ that are plotted vs. c in Figure 10. A reasonable straight line passing through the origin is obtained, and the derived value of k_O is listed in Table II. The good straight lines obtained in Figures 8–10, and the good agreement among the kinetic parameters deriving from the different experiments

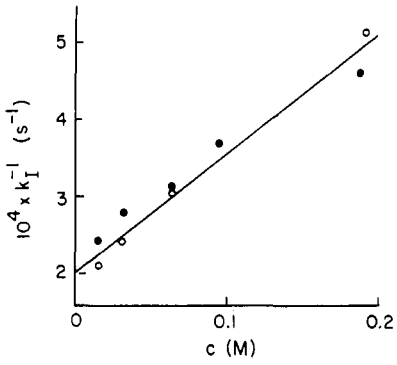

FIGURE 9: Plots of k_I^{-1} vs. c for the racemization of L-proline (●) and of D-proline (○). The values of k_I^{-1} derive from the data of Figure 8. Only reactions where c is ≥15.6 mM are plotted.

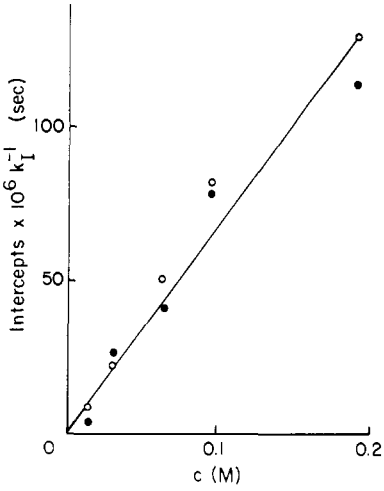

FIGURE 10: Plot of the intercepts from Figure 8 divided by the appropriate k_I vs. c. The values of k_I derive from the gradients of the lines in Figure 8. Only reactions where c is ≥15.6 mM are plotted. Data for L-proline (●) and D-proline (○) are shown.

summarized in Table II, confirm the phenomenon of oversaturation and its theoretical description. It is evident that eq 18 correctly describes the observed variation in the optical rotation with time at all substrate concentrations and that k_I varies with substrate concentration as described by eq 12.

The existence of three different kinetic regimes can be illustrated most clearly by plotting the logarithm of the first-order rate constant k_I vs. the logarithm of the total substrate concentration (c). This is shown in Figure 11. The bell-shaped curve of Figure 11 shows the variation in k_I calculated from eq 12 and the data in Table III. Since unsaturated terms are not completely negligible for the analysis of the oversaturated data and vice versa, we can make the small necessary corrections to obtain the values of the kinetic parameters given in Table III. The straight lines in Figure 11 are calculated from the parameters in Table III and show the behavior of each of the three terms in eq 12 that contribute to k_I. At low values of c, in the *unsaturated* region, k_I is proportional to c and k_I^{-1} is dominated by the term $2/(k_U c)$. At higher values of c, in the *saturated* region, k_I becomes independent of c and k_I^{-1} is dominated by the term $(1/k_{cat^+} + 1/k_{cat^-})$. Finally, at very high values of c, in *oversaturation*, the last term of eq 12 $[c/(2k_O)]$ dominates k_I^{-1}, and k_I *falls* with increasing substrate concentration. Since we know all the kinetic constants in eq 12, it is possible to calculate for any substrate concentration the relative contribution of each set of terms to k_I.

The intersections of the straight lines in Figure 11 are the two "switch concentrations" (Albery & Knowles, 1986), c_P and

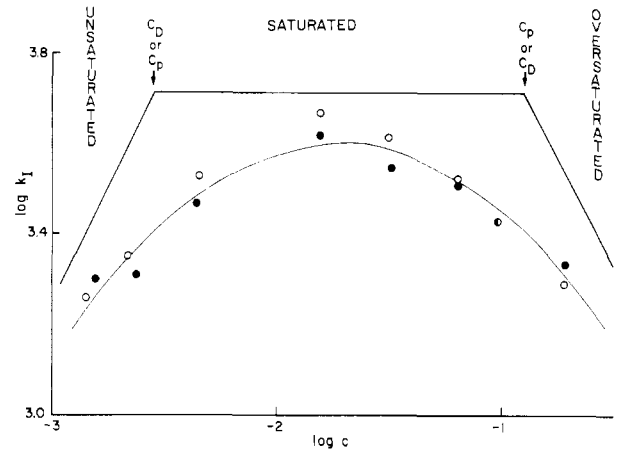

FIGURE 11: Double logarithmic plot of log k_I vs. log c. The values of k_I derive from the plots in Figures 6 and 8. Data for L-proline (●) and D-proline (○) over the whole concentration range (1.58–191 mM) are plotted.

Table III: Kinetic Parameters for the Interconversion of L- and D-Proline Catalyzed by Proline Racemase[a]

parameter	value
k_U (M^{-1} s^{-1})	9.0×10^5
$k_{cat^+}^{-1} + k_{cat^-}^{-1}$ (s)	7.7×10^{-4}
$k_{cat^+} = k_{cat^-}$ (s^{-1})	2600
k_O (M s^{-1})	81
c_D or c_P (mM)	2.9
c_P or c_D (mM)	125

[a] These values are derived from those in Table II after allowing for the small effects of the unsaturated terms in the oversaturated region and vice versa [see Albery & Knowles (1986)].

c_D, which divide the diagram into the three kinetic regimes. At low substrate concentrations, under unsaturated conditions, the most stable form of the enzyme is unliganded, and the reaction rate is limited by the conversion of a free enzyme form (e.g., E_1 + S) to a bound transition (e.g., transition state 2) as shown in Figure 3. As the concentration of substrate increases, the system moves into the saturated regime, and the most stable enzyme form may become E_1S. The rate-limiting conversion is now (as illustrated for bound state saturated in Figure 3) from a bound enzyme state (E_1S) to a bound transition state (2). The substrate concentration at which this switch occurs, when the free energies of E_1 + S and E_1S, for example, are equal, is called the "dip-switch concentration", c_D. For a racemase (for which $K_{S,P}$ = 1), we have shown (Albery & Knowles, 1986) that

$$c_D = \frac{2(1 + K_4^{-1})}{K_1 + K_{1,2}} = \frac{2(1 + K_4)}{K_3^{-1} + K_{2,3}^{-1}} \qquad (23)$$

Alternatively, saturated behavior may arise because of a switch in the rate limiting transition state, where (as illustrated for free-state saturation in Figure 3) the rate-limiting step becomes the interconversion of two forms of the free enzyme (e.g., E_2 over transition state 4). The substrate concentration at which this switch occurs is when the free energies of transition states 2 and 4, for example, are equal, and is called the "peak-switch concentration", c_P, for which we have shown (Albery & Knowles, 1986)

$$c_P = \frac{2k_4}{k_{-3,2,1}} = \frac{2k_{-4}}{k_{1,2,3}} \qquad (24)$$

When $c_D < c_P$, the saturated regime is bound state saturated, and when $c_P < c_D$, the saturated regime is free state saturated. From eq 8, 9, 13, 14, and 24, as described in the Appendix, we can show that

$$\frac{c_P}{2k_O} + \frac{2}{k_U c_P} = \frac{1}{k_{cat^+}} + \frac{1}{k_{cat^-}} \quad (25)$$

This quadratic equation might suggest that c_P can be found from the kinetic parameters reported in this paper. Unfortunately, however, as discussed elsewhere (Albery & Knowles, 1986), using eq 8, 9, 13, 14, and 23, as described in the Appendix, we find that c_D obeys exactly the same quadratic equation! We cannot, therefore, tell which root of eq 25 is c_P and which is c_D. Thus, the experiments reported in this paper reveal the existence of three kinetic regimes (unsaturated, saturated, and oversaturated) and determine the two switch concentrations at 2.9 and 125 mM. We cannot define which of the two switch concentrations is which, and, therefore, we cannot define the nature of the saturated regime. This important distinction is made from the results of the experiments reported in the following paper (Fisher et al., 1986).

APPENDIX

In this Appendix, we derive eq 25 from eq 8, 9, 13, 14, and 24. On the left-hand side of eq 25, from eq 13 and 24

$$\frac{2}{k_U c_P} = \frac{1 + K_4^{-1}}{k_{-4}} = \frac{1}{k_4} + \frac{1}{k_{-4}} \quad (26)$$

From eq 14 and 24

$$\begin{aligned} \frac{c_P}{2k_O} &= \frac{K_3^{-1} + K_{2,3}^{-1}}{k_{-3,2,1}} \\ &= (K_3^{-1} + K_{2,3}^{-1})\left(\frac{1}{k_{-3}} + \frac{K_3}{k_{-2}} + \frac{K_{2,3}}{k_{-1}}\right) \\ &= \frac{1}{k_3} + \frac{1}{K_2 k_3} + \frac{1}{k_{-2}} + \frac{1}{k_2} + \frac{K_2}{k_{-1}} + \frac{1}{k_{-1}} \\ &= \frac{1}{k_3} + \frac{1}{k_{2,3}} + \frac{1}{k_{-1}} + \frac{1}{k_{-2,1}} \end{aligned} \quad (27)$$

Addition of the terms on the left-hand side of eq 25, given by eq 26 and 27, gives the same result as addition of $1/k_{cat^+}$ and $1/k_{cat^-}$ given by eq 8 and 9.

Replacing eq 24 for c_P by eq 23 for c_D, we find that c_D obeys the *same* quadratic expression as that given in eq 25. From eq 14, 23, and 26 we find that

$$\frac{c_D}{2k_O} = \frac{1 + K_4}{k_4} = \frac{2}{k_U c_P} \quad (28)$$

Substitution in eq 25 then shows that c_D obeys the same quadratic equation as c_P.

Registry No. L-Proline, 147-85-3; D-proline, 344-25-2; proline racemase, 9024-09-3.

REFERENCES

Albery, W. J., & Knowles, J. R. (1976) *Biochemistry 15*, 5631–5640.

Albery, W. J., & Knowles, J. R. (1986) (submitted for publication).

Cardinale, G. J., & Abeles, R. H. (1968) *Biochemistry 7*, 3970–3978.

Cleland, W. W. (1963) *Biochim. Biophys. Acta 67*, 104–137.

Fisher, L. M., Albery, W. J., & Knowles, J. R. (1986) *Biochemistry* (second paper of seven in this issue).

Hohorst, H. J., Reim, M., & Bartels, H. (1962) *Biochem. Biophys. Res. Commun. 7*, 137–141.

Rudnick, G., & Abeles, R. H. (1975) *Biochemistry 14*, 4515–4522.

Sacktor, B., & Wormser-Shavit, E. (1966) *J. Biol. Chem. 241*, 624–631.

Swingle, S. M., & Tiselius, A. (1951) *Biochem. J. 48*, 171–174.